Sensitivity analysis of the parameters for assessing a hygrothermal transfer model HAM in bio-based hemp concrete material

Maroua Benkhaled, Salah-Eddine Ouldboukhitine, Amer Bakkour, Sofiane Amziane

Version of Record: https://www.sciencedirect.com/science/article/pii/S0735193322000069
Manuscript_04f51593910c8f3e4f943963c4376143

Sensitivity analysis of the parameters for assessing a hygrothermal transfer model HAM in bio-based hemp concrete material

Maroua Benkhaled [1], Salah-Eddine Ouldboukhitine [1], Amer Bakkour [2] and Sofiane Amziane [1,*]

[1] Université Clermont Auvergne, CNRS, SIGMA Clermont, Institut Pascal, F-63000 Clermont-Ferrand, France
[2] Department of Physics, Faculty of Sciences, Lebanese University, Lebanon
* Corresponding author: sofiane.amziane@uca.fr

Abstract

In order to better predict the hygrothermal behavior of porous building envelopes, it is essential to develop reliable mathematical models which accurately capture the coupled heat, air, and mass (HAM) transport and its influence on the indoor atmosphere. Recently, numerous models have been developed to predict the performance of bio-based building envelopes. However, the large number of input parameters and lack of knowledge of the intrinsic characteristics of the materials mean these models are quite difficult to implement. To determine the most influential hygrothermal parameters for a hemp concrete wall, a sensitivity study was conducted on the input parameters, based on the probability density distribution of Gaussian centered law; the results are presented herein. A reduced model was developed by eliminating the parameters with little or no influence on HAM transfer. Then, a dimensionless study of the reduced model was carried out. This generated an indicative parameter ς, which can be used to classify building materials and identify the most suitable. In MATLAB software, the simulated results for a hemp concrete wall showed satisfactory concordance with the experimental results found in the literature. The temperature profiles are accurately estimated. Note that the model must always take account of the evolution of water content to ensure accurate RH predictions.

1. Introduction

The external surfaces of building envelopes are constantly subject to numerous environmental stresses. These stresses cause heat, air, and moisture to be transported through the wall. To predict certain aspects of building performance, such as indoor air quality, structure durability, moisture growth, and energy consumption, one must carefully assess coupled HAM transfer in porous building materials.

Over the years, a variety of models and simulation tools have been developed to predict the hygrothermal behavior of porous building materials. Mostly, these focus on heat and moisture transport [1]–[11]. Recently, in view of the significant impact of air on heat and moisture transport through lightweight constructions, a great deal of effort has been invested in developing coupled HAM models based on numerous mathematical models and discretization techniques for numerical approximation [12]–[25].

However, it is often difficult to put these models into practice, due to lack of knowledge of the intrinsic characteristics of the materials under study. A further complicating factor is the large number of input parameters, which often cannot easily be measured either analytically or experimentally, because they are strongly interconnected and vary simultaneously. Experimental measurement of these parameters may give rise to errors, which may influence predictive performance. Moreover, early models have not ranked the parameters by their degree of influence on hygrothermal transfer. Consequently, a number of researchers have applied parametric sensitivity criteria to improve numerical estimations of both temperature and RH (relative humidity), as far as possible [26]–[43]. Other researchers applied a scale analysis study to simplify the physics parameters to identify the dominant sources of transfer [44]- [45].

For instance, In the study of Seng et al. [44], the heat and moisture transfer model through hemp concrete was studied based on experimental data. A scale analysis was applied to simplify the set of equations describing the physics by providing, in an order of magnitude sense, the dominant sources of transfer. For different classes of relative humidity, the material was submitted to a variation in temperature and relative humidity on its surface. The results show a significant change around a relative humidity of 95%. It was concluded through this study that the dominant mechanism becomes the capillary pressure gradient for this case of high relative humidity. In the latter relative humidity range, phase change enthalpy becomes in the same order of magnitude as conduction heat transfer.

In another research work of Seng et al. [45], the behavior at wall scale of a hemp-based hygroscopic material under various temperature and moisture dynamic conditions was studied through numerical and experimental study using a climatic chamber. The performed experiment demonstrated the coupling effect of heat and moisture transport phenomena and how a temperature difference can be a sufficient driving force for the release of moisture. The impact of moisture adsorption on heat release and on the temperature changes within the wall was also pointed in this study. The numerical study highlighted the moisture dumbing capability of the material and its thermal insulation capacity.

Mendes et al. [26] applied parametric sensitivity to their model, which is based on Phillip and De Vries' model, to reduce computational time. Different simplified sub-models are defined, in which specific transport coefficients are set as constant or disregarded to evaluate their influence on predicting loads in porous walls. They found that neglecting moisture transfer led to an underestimation of the yearly integrated heat flux by up to 59%, which skewed the estimation of the building's energy consumption.. Bart et al. [27] carried out a sensitivity study on Kunzel's model to assess the impact of uncertainties in physical properties for a hemp concrete wall. The distributions of RH and temperature within hemp concrete in the reference case are compared to cases with properties altered by ±20%. This change in dry density, thermal conductivity, and heat capacity produces no significant differences in terms of temperature and RH distributions with the reference case. Similar results were found by Olutimayin and Simonson [28] for cellulose insulation, with shifts of ±5%, and by Van Belleghem et al. [29] for gypsum board.

However, changing the vapor resistance factor or sorption isotherm by ±20% has major impacts on the RH profiles and a negligible effect on the temperature fields. Oumeziane et al. [30] presented the impact of density and hysteresis on hygrothermal transfer in a hemp concrete wall, based on Kunzel's model. By applying different conditions, the work showed that these parameters influence both the theoretical temperature and RH profiles. Othmen et al. [31] studied the influence of the input parameters of the Kunzel model using local sensitivity analysis (LSA). The parametric analysis was applied on two single-layer walls made of limestone and hemp concrete, by varying the hygrothermal properties of the materials, the surface transfer coefficients and the initial conditions by 5%.

In these studies of the parametric sensitivity of hygrothermal models, the authors consider a representative range of variation of the input parameters/ conditions with respect to their reference values. In addition, some parameters were set as constant, such as sorption capacity and thermal conductivity.

In this paper, to more precisely evaluate the influence of input parameters on the findings of hygrothermal transfer in building envelopes, a sensitivity study is carried out based on the probability density distribution described by a beta law defined by two parameters of form, α and β. This distribution is bounded based on variation intervals for each input parameter, in accordance with all values found in the literature. The work starts with a sensitivity analysis on a bare hemp concrete wall. Using MATLAB, the parameter values are randomly chosen from the beta distribution. The correlation between parameters and driving transfer potentials is determined by the slope coefficient of variation of inflection points. The present method is different from the one applied in the study of Seng al [44]- [45] where a scale analysis was applied by submitting the material to a variation in temperature and relative humidity on its surface. The two methods are complementary and lead to similar results. After the sensitivity study, a reduced model is developed by eliminating the parameters with little or no influence on HAM transfer. Next, a dimensionless study of the reduced model is conducted. This study identifies dimensionless thermal and hydric coefficients that give an indication of wall performance (thermal insulation and hygric regulation). From these two coefficients, a factor ς is identified to classify building materials in order to identify the most suitable. Then, the simulated results of the reduced model are compared to the experimental results found in the literature for hemp concrete walls. In addition, the developed reduced model is applied to cellular concrete to test its validity for dealing with different building materials. Finally, the reduced model is used to predict the hygrothermal behavior of a hemp concrete wall subjected to the stresses generally encountered in the building sector (winter, summer, and day-to-day stresses).

2. Modeling of coupled heat, air and moisture transfer in building envelopes

Several models of heat, air and moisture transfer were provided in the literature by Luikov [46], Whitaker [47] and Philip and De Vries [48]. These proposed models were adapted to building materials [49], [50]. The model of Philip and De Vries [48] is considered in the present work for

predicting the hygrothermal behavior of hemp concrete. This model considers that the moisture transport occurs under two phases (liquid and vapor). The following assumptions were made:

1. The phases (solid, liquid and gas) present are in local thermodynamic equilibrium.
2. The solid medium is undeformable.
3. The gas phase obeys the ideal gas law.
4. Radiative heat transfer is negligible.
5. Moisture transfer under the influence of gravity is negligible.

The model considers temperature T [K], water vapor pressure P_v [Pa], and total pressure P [Pa] as driving potentials of heat, hydric, and air transfer, respectively. In addition, this model takes account of the variation of hygrothermal material parameters depending on water content and temperature, to improve the accuracy of the study.
The following coupled equations represent the energy, air, and mass balances, respectively. The heat transfer is expressed by considering transfer by conduction and advection due to water vapor and total pressure gradients:

$$\boldsymbol{C_p\,\rho_s\,\frac{\partial T}{\partial t} = div(\lambda \nabla T + \alpha\,\nabla P_v + \gamma \nabla P) + L_v\,\rho_s \sigma\,C_m\,\frac{\partial P_v}{\partial t}} \quad \text{Eq. 1}$$

$$\boldsymbol{C_a\,\frac{\partial P}{\partial t} = div\left(K_f \nabla P\right)} \quad \text{Eq. 2}$$

$$\boldsymbol{C_m \rho_s\,\frac{\partial P_v}{\partial t} = div\left[K_m \nabla P_v + K_T\,\nabla T + K_f \nabla P\right]} \quad \text{Eq. 3}$$

The material properties are: heat capacity C_p [J/kg.K], density ρ_s [kg/m^3], thermal conductivity λ [w/m.K], heat transfer coefficient by advection due to the water vapor pressure gradient α [m²/s], heat transfer coefficient by advection due to the total pressure gradient γ [m²/s], latent heat L_v [j/kg], phase-change criteria $\sigma = {div(j_v)}/{div(j_m)}$ [-], moisture storage capacity $C_m = ({1}/{P_{vsat}}).({\partial\omega}/{\partial\varphi})$ [kg/kg.Pa], humid air capacity C_a [s²/m²], total infiltration coefficient K_f [kg/(m.s.Pa)], total moisture permeability K_m [kg/(m.s.Pa)], and liquid water conductivity K_T [kg/m.s.K].

So that the model can be used with confidence, both analytical and experimental validations have been carried out for a hemp concrete envelope, on a one-dimensional case, using the finite element method implemented in MATLAB. This method relied on the extensive programming freedom and high level of parameter visualization, since the solving methodologies found in the literature are used as black boxes, having predefined equations that require no intervention from the user in the resolution process. The simulated results showed satisfactory agreement with one-dimensional numerical benchmark case N°2 [51] and experimental results found in the literature [52]. The evolution of temperature and relative humidity profiles within the hemp envelope were predicted accurately with the finite element method. This concordance showed the efficiency of the numerical resolution software MATLAB.

These coupled HAM equations show wide variability of the measured material parameters involved in the hygrothermal transfer. These parameters are strongly related and often cannot be easily measured, making the implementation of this transfer model more difficult. Therefore, a sensitivity study of parameters is conducted in order to address such a problem.

3. Sensitivity analysis of the HAM model

After the HAM model was validated with satisfactory results compared to the results found in the literature, we conducted a sensitivity study of the model parameters in order to study the influence of each on the hygrothermal transfers in building envelopes. The sensitivity study depends on determining the change in output data as the result of variations in input data. Generally, sensitivity study of the input parameters for a coupled heat, air, and moisture transfer modeĺ consists of varying one parameter relative to a reference value and keeping the others the same. In reality, these parameters are strongly related and vary at the same time. Thus, some parameters cannot be found analytically or experimentally. From this viewpoint, it will be interesting to conduct a sensitivity study of parameters to evaluate their influence on the hygrothermal behavior. It can simplify the number of input parameters which have little or no influence on hygrothermal transfer. This study focuses on a bare hemp concrete wall. Indeed, the sensitivity study is based on the probability density distribution of a centered Gaussian law. This distribution is bounded and defined on a variation interval for each of the hygrothermal properties (input parameters). The distribution is described by a beta law, defined by two parameters of form, typically written as α and β (in our case, α=β=2). The choice of this approach is due to the major disparity of the hygrothermal properties imposed by the morphological structure of hemp concrete. In this approach, the variation intervals of each input parameter to the model are estimated according to all the values found in the literature for bio-based materials. The variation intervals of the input parameters for a density ρ = 450-550 kg/m^3 are presented in **Table 1**.

Table 1: The characteristic of the distribution function Beta: Mean μ, standard deviation σ and the interval distribution

Material properties	Variation interval	μ	σ
λ [W.m^{-1}.K^{-1}]	[0.05 0.15]	0.01	0.015
C_p [J.kg^{-1}.K^{-1}]	[1000 1500]	1250	100
K_f [kg.m^{-1}.s^{-1}.Pa^{-1}]	[5. 10^{-12} 4. 10^{-11}]	2.25. 10^{-11}	0.6. 10^{-11}
C_a [s^2.m^{-2}]	[5. 10^{-5} 4.5. 10^{-4}]	2.5. 10^{-4}	0.6. 10^{-4}
K_m [kg.m^{-1}.s^{-1}.Pa^{-1}]	[1. 10^{-12} 9. 10^{-11}]	4.5. 10^{-11}	1. 10^{-11}
C$_m$ [kg.kg^{-1}.Pa^{-1}]	[5. 10^{-6} 4. 10^{-4}]	5. 10^{-5}	1. 10^{-5}
σ [-]	[0.8 1]	0.9	0.05
α [m^2.s^{-1}]	[1. 10^{-8} 4. 10^{-4}]	5. 10^{-5}	1. 10^{-5}
γ [m^2.s^{-1}]	[1. 10^{-8} 4. 10^{-6}]	5. 10^{-7}	1.5. 10^{-7}

K_T [kg.m^{-1}.s^{-1}.K^{-1}]	[1. 10^{-16} 4. 10^{-14}]	5. 10^{-15}	1. 10^{-15}

10,000 values of input parameters are randomly selected from each Gaussian centered distribution. This value represents the number of iterations defined by the counter m in MATLAB. For each iteration, the coefficients of the model take a new arbitrary value from within its interval. The goal is to determine the correlation between the parameters of the model at the input and the transfer motors at the output. This method allows us to determine the influence of each coefficient on the hygrothermal transfer in a hemp concrete wall and to simplify the HAM model. The study configuration, in 3 positions and treated for 20 days, consists of applying a T and RH gradient on a hemp concrete wall (**Figure 1**).

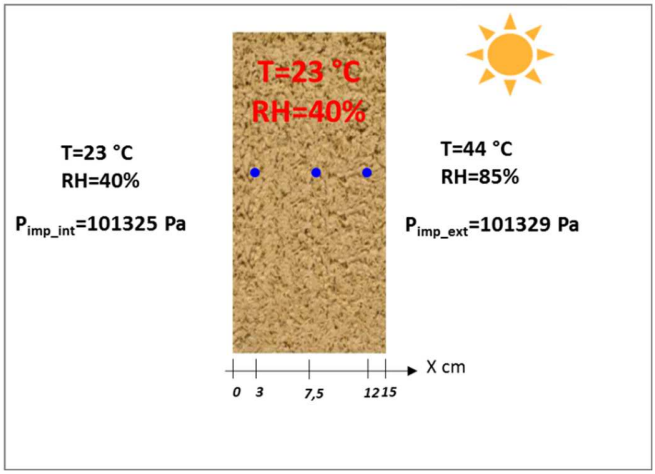

Figure 1: The study configuration

For each iteration, we obtain an evolution of temperature T, vapor pressure P_v and gas pressure P_g, during the simulation time at different mesh nodes. For this purpose, we fix our spatial counter in the middle of the wall (i=n/2) to observe the changes in the material's response over time at each iteration. At each iteration, we detect a representative point on each profile curve of T, P_v, and P_g, called the inflection point (**Figure 2**), on which the sensitivity analysis is based. Yet if we vary all values of one parameter at the same time, the inflection point varies 10,000 times according to the number of iterations and forms a cloud of points. For instance, the inflection points of temperature, vapor pressure and gas pressure as a function of the variability of the thermal conductivity are shown in **Figure 3**. Therefore, there is obviously a correlation between the temperature and the conductivity determined from the slope coefficient of the red line representing the correlation value, whereas, for vapor and gas pressure, there is no correlation (the slope coefficient is null).

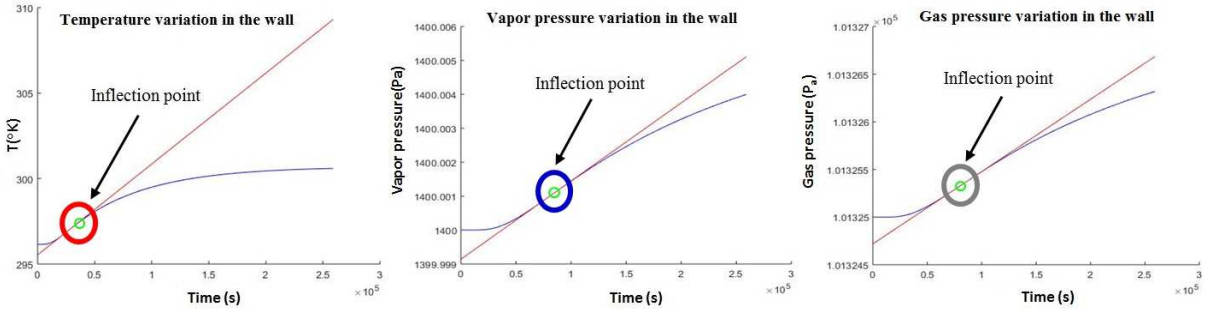

Figure 2: The inflection points of T, P_v and P_g when thermal conductivity is varied

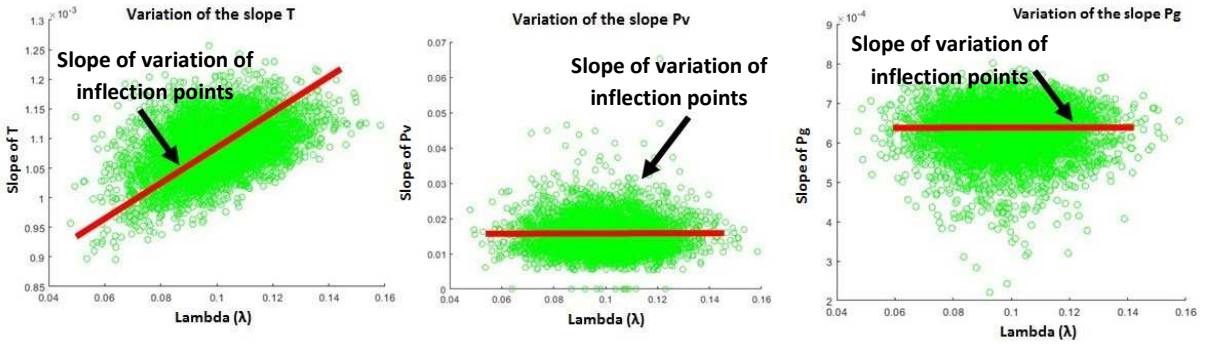

Figure 3: Cloud of inflection points of T, P_v, and P_g when thermal conductivity is varied

The shape of this cloud reflects the impact of the random variation of the input parameters of the model on the evolution of T, P_v, and P_g. For this reason, we determine the correlation which represents the slope of the trend lines of each cloud of points. Thus, through correlation value, we deduce the impact of the hygrothermal properties on the hygrothermal behavior of hemp concrete (**Figure 4**).

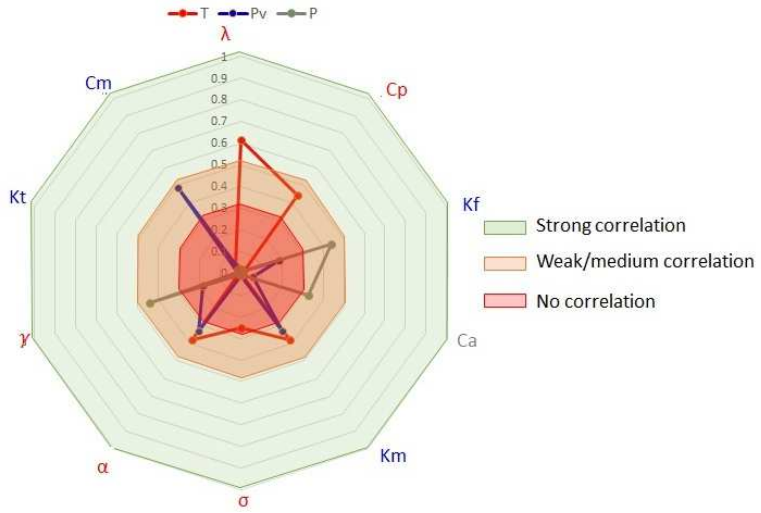

Figure 4: Correlation between the outputs (T, Pv, P) and the inputs (the hygrothermal properties)

Figure 4 classifies the hygric and thermal properties according to their influence on the hygrothermal behavior. This is reflected in the correlation rate which varies between 0 and 1. The most influential parameters on the hygrothermal behavior have a correlation rate that tends towards 1. For instance, if we look at the evolution of the temperature (red line), we find a correlation with thermal conductivity λ and calorific capacity Cp, but also see a correlation with the parameter Km which represents the water vapor permeability. Therefore, some parameters do not influence the hygrothermal transfers. This study allows us to simplify the HAM model by eliminating the parameters with low correlation (less than 0.3). We also note that in construction, the gas pressure gradients are small, so the gas transfer equation can be eliminated from the HAM model. On this basis, we distinguish the four most influential parameters on heat and mass transfer: thermal conductivity λ, specific heat C_p, water storage capacity C_m, and water vapor permeability K_m.

Where we started with a system of three equations with twelve parameters, we finally end up with a simple system of two coupled equations with six parameters, called the "Reduced Model" (R.M):

$$\begin{cases} C_p\rho_s \dfrac{\partial T}{\partial t} = div[\lambda \nabla T] + L_v\rho_s C_m \dfrac{\partial P_v}{\partial t} & \text{Eq. 4} \\ \rho_s C_m \dfrac{\partial P_v}{\partial t} = div[K_m \nabla P_v] & \text{Eq. 5} \end{cases}$$

Therefore, this reduced model will be the subject of a dimensionless study that consists of separating the variables. The transfer motors will be the position, time, temperature, vapor pressure, and the hygrothermal parameters as a function of the base unit. This reduced model yields satisfactory results with reduced computation times.

4. Dimensionless study

Often, the dimensionless approach can greatly simplify a model by providing indicative parameters for transfer phenomena. Indeed, the dimensionless study is a procedure whereby units can be removed from an equation by appropriate substitution of parameters and normalization of variables to simplify the parametric representation of physical problems. This approach aims to reduce the computation time by reducing the number of parameters and provide indicators able to establish a correlation between thermal insulation and water regulation from the most influential hygrothermal properties. Until recently, few dimensionless studies on hygrothermal transfer models have been reported [47]–[54]. However, these case studies were elaborated by introducing dimensionless numbers such as Biot *(Bi)*, Posnov (*Pn*), Peclet (*Pe*), Kossovitch (*Ko*) and Luikov (*Lu*). Thus, the present dimensionless study proposes new scale numbers that are attributed to a combination of the hygrothermal parameters of the studied material. *Table 2* presents the parameters and variables of the problem and their appropriate base units.

Table 2: Base units of variables and parameters

Variables		Parameters	
P_v	$[M.L^{-1}.T^{-2}]$	C_m	$[M^{-1}.L.T^{2}]$
T	[Θ]	C_p	$[L^{2}.T^{-2}.\Theta^{-1}]$
X	[L]	K_m	[T]
t	[T]	L_v	$[L^{2}.T^{-2}]$
		Λ	$[M.L.T^{-3}.\Theta^{-1}]$

A new nomenclature is proposed to identify the normalized variables. The variables were normalized by dividing each by a scale number with the same unit, such that:

$$\tau = \frac{t}{t_c}; \chi = \frac{x}{x_c};\ \tilde{P_v} = \frac{P_v}{P_{vc}};\ \tilde{\theta} = \frac{T}{T_c}$$

with the scale numbers:

$$t_c[s], x_c[m], P_{vc}[Pa], T_c[K]$$

Depending on the base unit, each of the scale numbers is attributed to a combination of the hygrothermal parameters of the studied material (in our case, hemp concrete) to obtain the same base unit (Table **3**).

Table 3*: Base unit of scale numbers*

Scale number	**Base unit**
$\boldsymbol{t_c} = \boldsymbol{k_m}$	$[T]$
$\boldsymbol{x_c} = \boldsymbol{k_m}\sqrt{L_v}$	$[L]$
$\boldsymbol{P_{vc}} = \frac{1}{C_m}$	$[M.\ L^{-1}T^{-2}]$
$\boldsymbol{T_c} = \frac{L_v}{C_p}$	[Θ]

Replacing each of these variables and parameters in the system of equations (Eq. 4 and Eq. 5), based on this new nomenclature, yields the following system:

$$\begin{cases} C_p\rho\dfrac{\partial(T_c\tilde{\theta})}{\partial(t_c\tau)} - L_v\,\rho\,C_m\dfrac{\partial(P_{vc}.\tilde{P}_v)}{\partial(t_c\tau)} = \lambda\dfrac{\partial^2(T_c\tilde{\theta})}{\partial^2(x_c.\chi)} & \text{Eq. 6} \\ \rho C_m\dfrac{\partial(P_{vc}.\tilde{P}_v)}{\partial(t_c\tau)} = K_m\dfrac{\partial^2(P_{vc}.\tilde{P}_v)}{\partial^2(x_c.\chi)} & \text{Eq. 7} \end{cases}$$

$$\begin{cases} C_p\rho\dfrac{T_c}{t_c}\dfrac{\partial\tilde{\theta}}{\partial\tau} - L_v\,\rho\,C_m\dfrac{P_{vc}}{t_c}.\dfrac{\partial\tilde{P}_v}{\partial\tau} = \lambda\dfrac{T_c}{{x_c}^2}\dfrac{\partial^2\tilde{\theta}}{\partial^2\chi} & \text{Eq. 8} \\ \rho\,C_m\dfrac{P_{vc}}{t_c}.\dfrac{\partial\tilde{P}_v}{\partial\tau} = K_m\dfrac{P_{vc}}{{x_c}^2}\dfrac{\partial^2\tilde{P}_v}{\partial^2\chi} & \text{Eq. 9} \end{cases}$$

$$\begin{cases} \rho\dfrac{C_p.K_m.L_v}{\lambda}\left[\dfrac{\partial\tilde{\theta}}{\partial\tau} - \dfrac{\partial\tilde{P}_v}{\partial\tau}\right] = \dfrac{\partial^2\tilde{\theta}}{\partial^2\chi} & \text{Eq. 10} \\ L_v\,\rho\,C_m.\dfrac{\partial\tilde{P}_v}{\partial\tau} = \dfrac{\partial^2\tilde{P}_v}{\partial^2\chi} & \text{Eq. 11} \end{cases}$$

By making the necessary simplifications and replacements, the reduced dimensionless system of the two parameters will be:

$$\begin{cases} \left[\dfrac{\partial\tilde{\theta}}{\partial\tau} - \dfrac{\partial\tilde{P}_v}{\partial\tau}\right] = \delta\dfrac{\partial^2\tilde{\theta}}{\partial^2\chi} & \text{Eq. 12} \\ \dfrac{\partial\tilde{P}_v}{\partial\tau} = \beta\dfrac{\partial^2\tilde{P}_v}{\partial^2\chi} & \text{Eq. 13} \end{cases}$$

with:

$\delta = \frac{\lambda}{\rho.C_p.K_m.L_v}$: Dimensionless thermal coefficient

$\beta = \frac{1}{\rho.C_m.L_v}$: Dimensionless hydric coefficient

These two coefficients give a representation of wall performance (thermal insulation and hygric regulation) and lead to an appropriate choice of building construction materials. Therefore, the approach adopted in this work consists of identifying an indicator from the most influential thermal and hygric properties on the hygrothermal response of building envelopes (thermal conductivity, specific heat, water storage capacity, and water vapor permeability). This indicator is obtained from a ratio of δ and β:

$$\varsigma = \frac{\delta}{\beta} = \frac{\lambda.C_m}{C_p.K_m}$$

Table 4 presents the hygrothermal properties of hemp concrete and other building materials (Cellular concrete, normal concrete and polystyrene).

Table 4: Comparison of hemp concrete with conventional materials

Parameter / Material	ρ	λ	C_p	C_m	K_m	ς
	kg/m^3	W/(m.k)	(j/kg.k).m	kg/kg.Pa	kg/(m.s.Pa)	-
Hemp concrete	320	0.091	1250	$2.14.10^{-5}$	1.10^{-10}	15.5792
Hemp concrete sealed with a waterproof film	320	0.091	1250	$2.14.10^{-5}$	1.10^{-12}	1557.92
Date palm concrete	954	0.185	1500	$8.57.10^{-6}$	$3.16.10^{-11}$	33.44
Cellular concrete	600	0.14	850	$1.07.10^{-5}$	$2.29.10^{-11}$	76.9586
Concrete C12/C25	2200	2	850	$1.42.10^{-5}$	$2.17.10^{-11}$	1539.71
Polystyrene	30.4	0.042	1500	$3.57.10^{-9}$	$1.87.10^{-12}$	0.05345

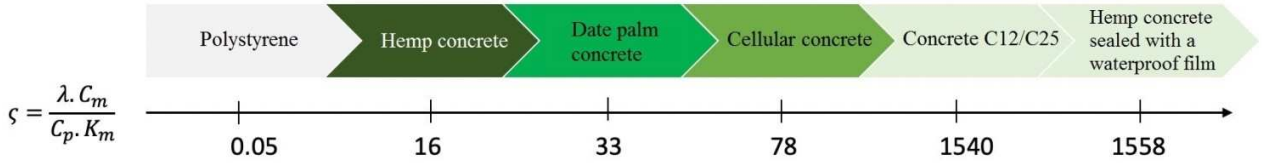

Figure 5: The evolution of ς as a function of construction materials

Figure 5 represents the classification scale of building materials depending on the value of the parameter ς. The two bio-based materials, hemp concrete and date palm concrete, sit between polystyrene and cellular concrete. On the other hand, this parameter has a high value for hemp concrete sealed with a waterproof film, so it behaves like normal concrete. Consequently, the indicator parameter ς links the thermal and the hygric performances of a material; $\varsigma \gg 1$ indicates the dominance of thermal diffusion and the insignificant contribution of mass transport at a macroscopic level in the hygrothermal transfer process. Indeed, under adiabatic conditions, this process is controlled by the evolution of heat by conduction. Indeed, this dimensionless indicator ς allowed us to select the most compatible building material to ensure a pleasant indoor environment while consuming less energy (thermal insulation and hygric regulation). Furthermore, hemp concrete is an ideal material for optimizing building envelope performance for a ς value between those of polystyrene and cellular concrete. The thermal and hygric qualities of a material expressed by ς can be associated with its MBV value to finally ensure hygroscopic properties which allow the material to absorb occasional surpluses of water vapor, without damage, and release it when conditions allow.

5. Experimental validation of reduced model

To validate the model of hygrothermal transfer in a hemp concrete building envelope, the results of the proposed model are compared to the experimental results found in the literature. The main objective of this comparison is to verify the reliability of the numerical resolution proposed by the simulation tool. For this purpose, two terms have been identified: a short term of 48 hours and a long term of 85 days. In both cases, a hemp concrete wall is exposed to simultaneous stresses of T and RH. The idea of applying these types of stresses is to estimate the hygrothermal behavior of the material before it reaches a quasi-steady state. This allows us to determine the material's intrinsic thermal and hygric characteristics.

5.1. Experimental validation of the model for a hemp concrete wall subjected to short static stresses of temperature and relative humidity

The first validation consists of comparing the numerical results of the developed model to the experimental data obtained by Samri [61]. The reason for this choice is the availability of input data necessary to feed our model and the proposed hygrothermal history. This history is based on so-called static stresses which correspond to constant temperature and relative humidity evolutions over each 24-hour period. Based on [61], we first present the validation of the model on a 30cm-thick unplastered hemp concrete wall. The climatic stress imposed on the chamber by Samri is shown in Figure **6**. This Dirichlet-type stress of temperature and humidity is applied on the external side of the wall. The study consists of simultaneously imposing levels of temperature and humidity. After stabilization at (23°C, 30%), the outdoor environment conditions are raised to (30°C, 70%) for 24 hours and then lowered to (20°C, 30%) at point E. The rise in temperature and relative humidity in the core of the wall during the first step is attributed to sorption. On the other hand, the interior side of the wall is in contact with the laboratory environment. It should be noted that for the latter, the hygrothermal conditions are not controllable, making it more difficult to numerically reproduce the hygrothermal behavior of the wall with MATLAB. In this case, it is assumed that the interior conditions are identical to the initial conditions of the wall, which is maintained at 23°C and 30% relative humidity. The simulation is carried out with a mesh size of 50 nodes and a time step size of 600s. The hygrothermal properties used in this case study are given in Table **5**. These parameters are used to feed our reduced model (R.M.) implemented in MATLAB.

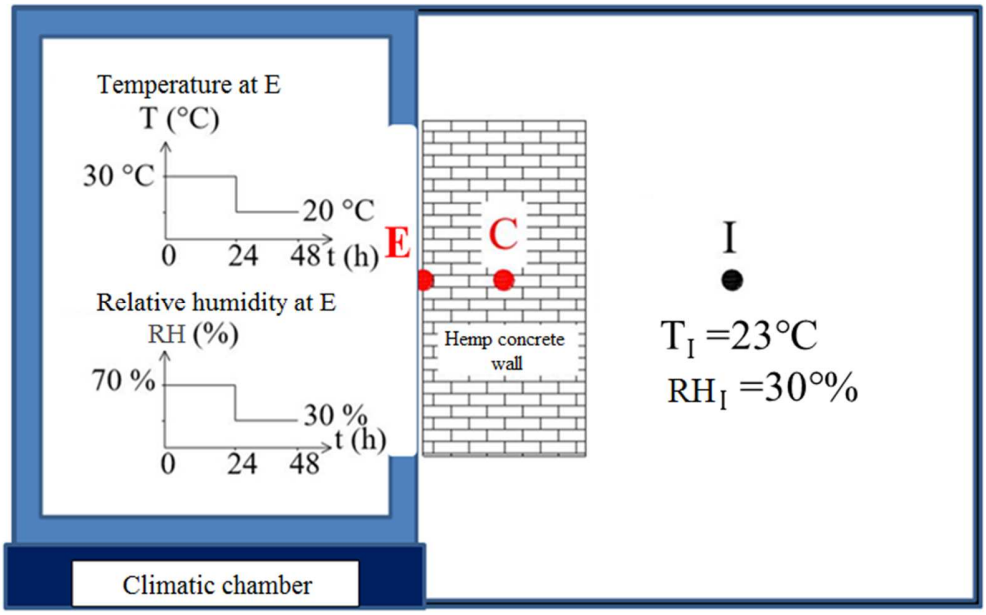

Figure 6: Configuration of the wall for study [61].

Material	**ρ**	**λ**	**C_p**	**K_m**	**C_m**
Hemp concrete (23°c, 30%)	kg/m^3	W/(m.K)	J/(kg.K)	kg/(m.s.Pa)	kg/kg.Pa
	329.7	0.088	1122.3	5.10^{-10}	$3.79.10^{-6}$

Table 5: Properties of hemp concrete for validation [61].

The hygrothermal behavior was modeled in the middle of the hemp concrete wall, at point C. The comparison of the numerical and experimental results is shown in **Figure 7** and **Figure 8**. Due to the static stress in E, the first sequence is 24 hours of adsorption, accompanied by a phase change. This leads to a rise in temperature due to condensation. Subsequently, a desorption phase manifests itself, when the relative humidity starts to decrease, continuing to do so until the 48-hour point. Thus, a drop in temperature is observed due to evaporation.

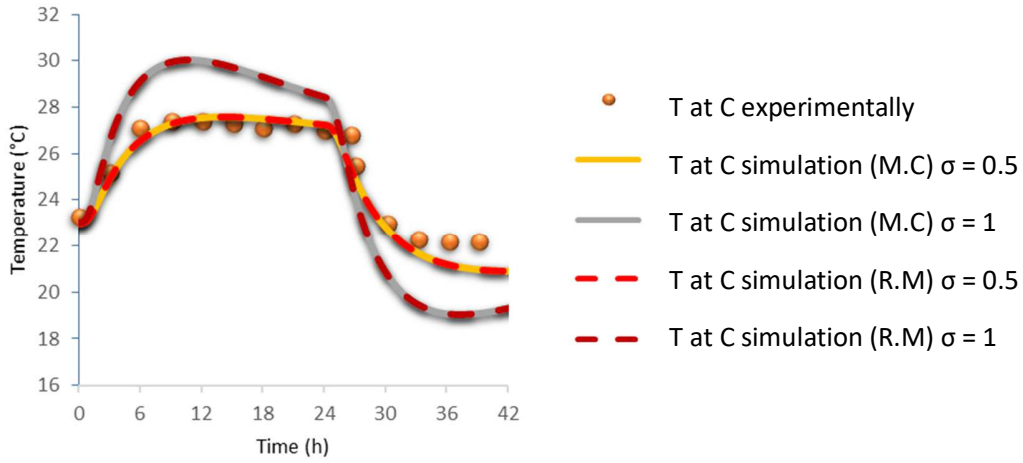

Figure 7: Comparison between experimental and numerical results of the temperature evolution at the center of the wall C.

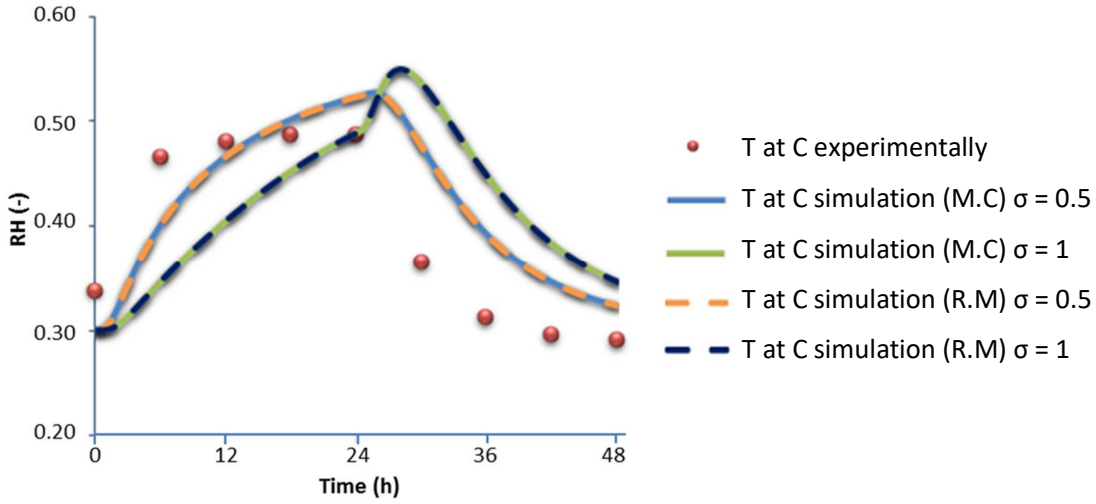

Figure 8: Comparison between the experimental and numerical results of relative humidity evolution at the center of the wall C.

For the hemp concrete wall, the numerical and experimental results conform when we consider that the mass exchange of water vapor represents half the total mass exchange ($\sigma = 0.5$). In this case, the evolution of T and RH obtained numerically over 48 hours at the center of wall C follows the same trend obtained experimentally in Samri's work. On the other hand, if we consider that the total mass transfer corresponds to mass exchange of water vapor ($\sigma = 1$), we observe a phase shift between the numerical and experimental results. Indeed, two temperature peaks are observed in the middle of the wall: a positive peak at the beginning of adsorption and a negative peak during desorption. These peaks are induced by condensation (exothermic) and evaporation (endothermic) within the material. These phenomena influence the distribution of water within the wall and create phase shifts related to the variation of relative humidity.

Therefore, it is necessary to consider the amount of water trapped in the pore network, so as to improve the numerical prediction of the hygrothermal behavior of a hemp concrete wall. This results in accurate modeling of the storage kinetics (hysteresis).

In conclusion, we noted significant agreement between the numerical and experimental results when we have an accurate estimation of σ. Hemp concrete is at half of its storage capacity when $\sigma = 0.5$, due to the adsorption and desorption cycles that occur before starting the experiment. Moreover, the numerical results are strongly impacted by the initial water content and its evolution in the wall because we are examining the hygrothermal behavior of partially saturated materials.

5.2. Experimental validation of the model for a hemp concrete wall subjected to long static stresses of temperature and relative humidity

The second investigation of the reduced model of the coupled heat and moisture transfers compares the numerical results obtained by MATLAB to the experimental results found on an unplastered hemp concrete wall by Leliévre [62]. The Dirichlet-type thermal and humidity stresses are applied to both sides of a 36cm-thick hemp concrete wall (Figure **9**), using a bi-climatic chamber (Figure **10**). Measurements are carried out with constant temperature conditions on one side (indoor environment) and variable temperature and humidity on the other (outdoor environment).

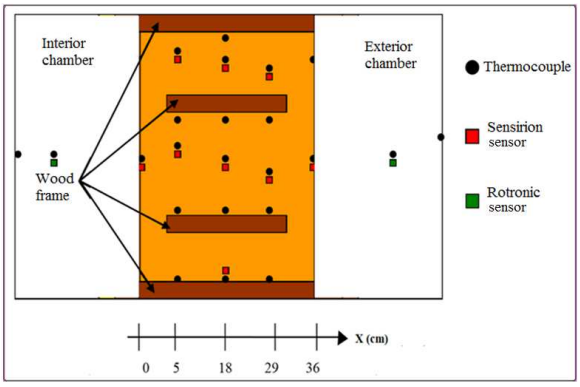

Figure 9: Study configuration [62]


Figure 10: Bi-climatic chamber [62]

The hygrothermal behavior of the unplastered hemp concrete wall is evaluated over 85 days, during which the temperature and relative humidity of the interior chamber are fixed at 24°C and 49%, while those of the exterior chamber vary in four successive phases (**Figure 11**). Each measurement sequence is about 20 days long, allowing the system to reach a quasi-steady state. For better numerical modeling with MATLAB, we endeavored to match the history of T and RH on the external side as closely as possible (**Table 6**).

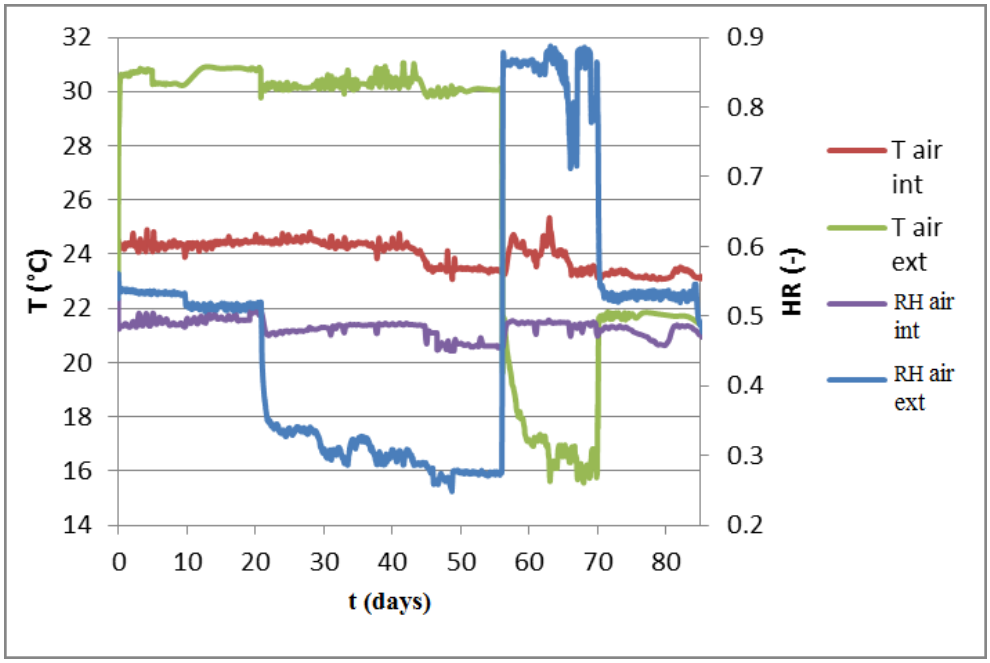

Figure 11: Experimental conditions of temperature and relative humidity [62].

	Initial condition	Indoor conditions	Outdoor conditions					
			Phase 1			Phase 2	Phase 3	Phase 4
	0>t	0<t<85 days	0<t<5 days	5<t<10 days	10<t<20 days	20<t<55 days	55<t<70 days	T>70 days
T (°C)	T_0=0.1398.x+ 24.389	24	30.7	30.2	31	30	0.045.t^2- 6.048.t+ 219.81	21.8
HR (-)	Pv_0=22.714.x +1548	0.49	0.54	0.51	0.5	9.10^{-5}.t^2- 0.0091.t +0.508	0.86	0.53

Table 6: Variations of outdoor and indoor T and RH as entered into MATLAB.

Before beginning the simulation, Leliévre monitored the temperature and relative humidity in the material, allowing them to stabilize. **Figure 12** shows the temperature and vapor pressure profiles at time t=5 days. The fact that these two profiles are linear, as well as the slight variations of temperature in the material between 5 and 20 days (Figure **13**), bear out the choice of the temperature and relative humidity in the material at t=5 days as initial conditions. Therefore, the simulation covers the period for which t is between 5 and 85 days. These two profiles of temperature T_0 and vapor pressure Pv_0 are described by two linear functions (equations 14 and 15) in the MATLAB code.

$$T_0 = 0.1398.x+24.389 \quad \text{Eq. 14}$$

$$Pv_0 = 22.714.x+1548 \quad \text{Eq. 15}$$

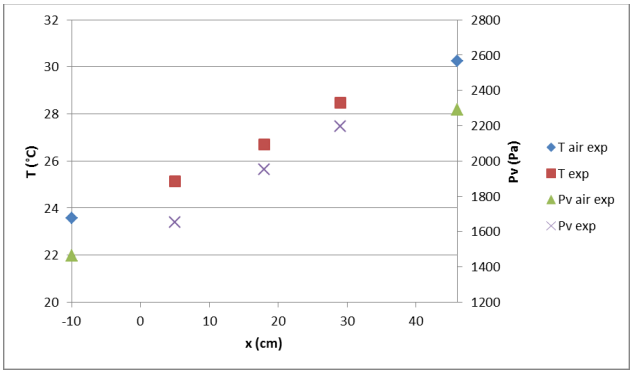

Figure 12: Initial temperature and vapor pressure profiles at t=5 days [62].

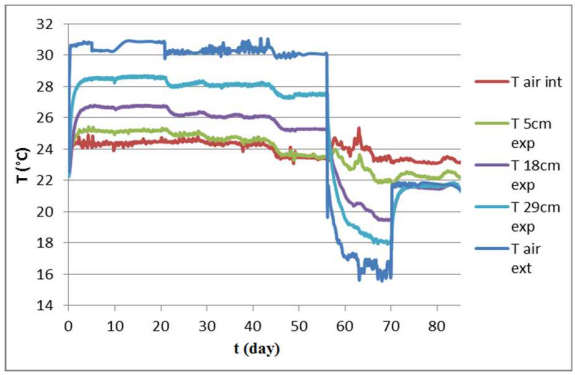

Figure 13: Measured temperatures in the material [62].

Results and discussion

In order to investigate the validity of our reduced model, we ran two confirmatory experiments: with and without taking the adsorption-desorption isotherm (Hysteresis) into account.

5.2.1 Results without taking the sorption isotherm into account

The first simulation is carried out without considering the evolution of the water content within the material. The reduced model implemented in MATLAB is used to numerically predict the hygrothermal behavior. A uniform mesh of 100 nodes is used, with a time step of 600s. The characteristics of the hemp concrete used in this study, based on the hygrothermal properties proposed by [62], are presented in Table **7**.

ρ	λ	C_p	K_m	C_m
$(kg.m^3)$	$(W.m^3K^{-1})$	$(J.kg^{-1}K^{-1})$	$(kg.m^{-1}.s^{-1}Pa^{-1})$	$(kg.kg^{-1}Pa^{-1})$
454	0.1166	1070	$3.71\ 10^{-11}$	$3.336\ 10^{-11}$

Table 7: Properties of hemp concrete input into MATLAB.

The results obtained by numerical simulation are compared to those found experimentally. Figures **14** and **15** show the simulated and measured T (°C) and RH profiles at three positions within the wall: 5cm, 18cm, and 29cm.

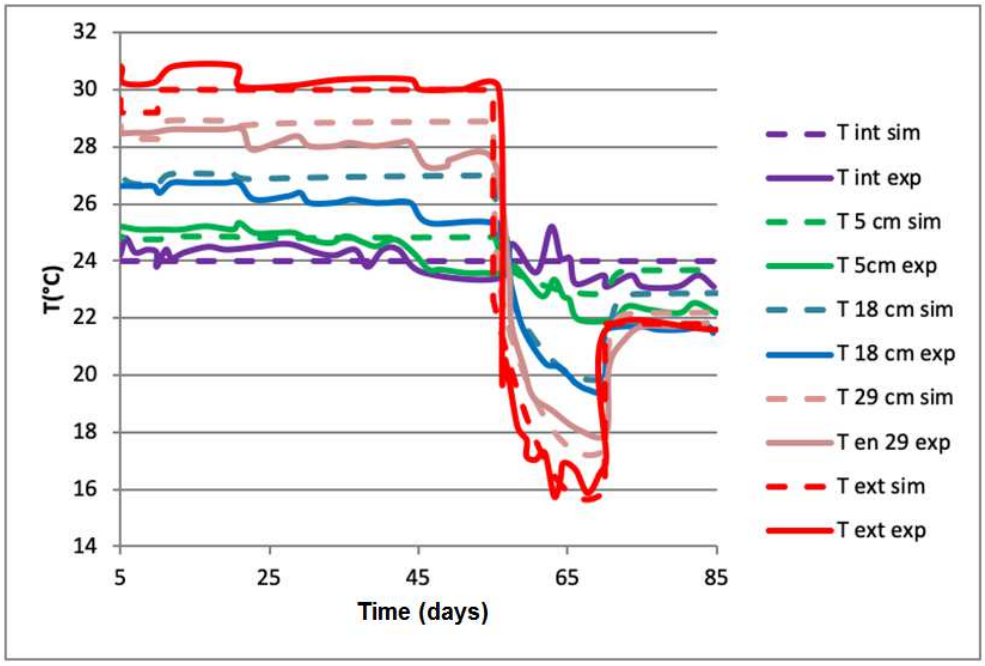

Figure 14: Simulated and measured temperatures.

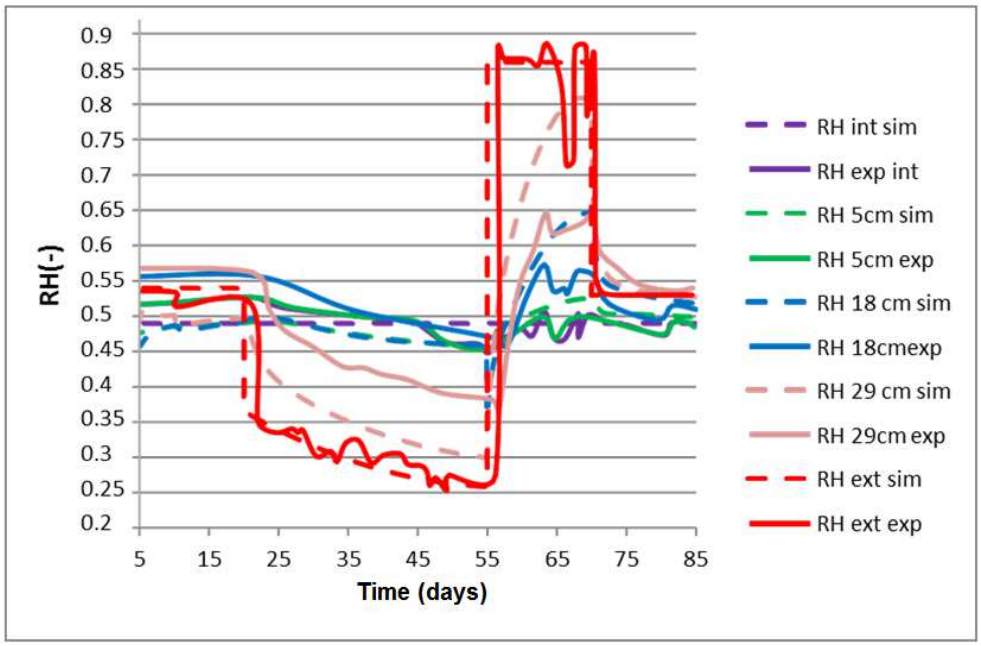

Figure 15: Simulated and measured relative humidity without considering the sorption isotherm.

The comparison between the numerical and experimental results of the temperature in the wall shows satisfactory accuracy. The temperatures at 29cm and 18cm reach a quasi-steady state during heating, with high values near the external temperature. On the other hand, the temperature variation at 5cm from the interior closely mirrors the set points imposed on the

interior side. This confirms the effectiveness of hemp concrete in attenuating external temperature variations and ensuring good thermal insulation for the interior environment.

As regards the relative humidity, the results show significant deviation between the simulated and measured RH, especially at 29cm, but at 5cm, the evolution of RH was close to the fluctuations imposed from inside. The difference is due to overestimation of the water transport in the wall. The water content distributed through the wall can affect the numerical responses.

Note that in the numerical results, we do not observe random fluctuations of indoor and outdoor temperatures and relative humidity, as observed in the experimental results, because we do not have access to the weather files used in this test.

5.2.2. Results taking the sorption isotherm into account

When studying the hygrothermal behavior of a porous wall, it is essential to consider the initial water content (W_{int}) and its variation within the wall. It is difficult to pinpoint the initial amount of water in the material. The water content of a porous material with hysteretic behavior cannot be evaluated independently of the material's hydric history. However, it is possible to deduce an approximate value from its history. In [62], Lelièvre started by saturating the hemp concrete with water, then dried it to 50% relative humidity. During this phase, the water content in the hemp concrete followed the main desorption curve $W(RH)=W_{des}(RH)$. On the other hand, the hemp concrete reached a minimum of 40% RH for the three measuring positions at 5cm, 18cm, and 29cm, owing to the uncontrolled fluctuations of the atmosphere in the vicinity of the wall. Therefore, for any RH greater than 40%, the water content of hemp concrete is between the curve reflecting the evolution of water content of primary adsorption from RH=40%, named $W_{ad,prim40\%}$ (RH), and the main desorption curve W_{des}. The initial values of water content in the wall for the two cases in question are represented by [62] in Figure **16**.

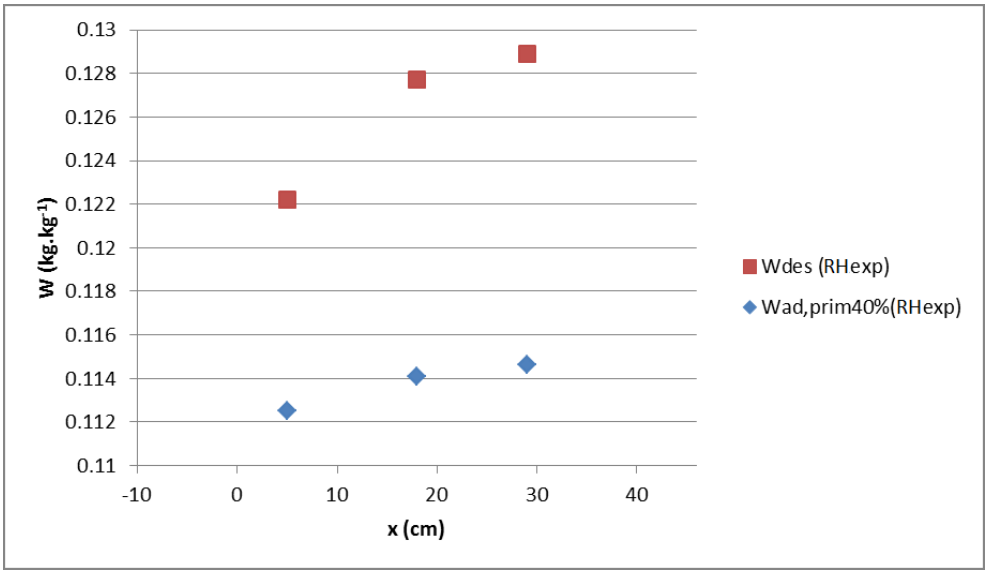

Figure 16: Initial water content profile [62].

From a numerical point of view, it is possible to create a fictional history to reproduce the humidity and temperature cycles experienced by the material. Based on the GAB model (Guggenheim, Anderson, and De Boer) whose coefficients are given by [62] in Table 8, we propose two curves: primary adsorption $W_{ad,prim40\%}(RH)$ and main desorption of hemp concrete.

$$W(RH) = \frac{W_m . C_{GAB} . K_{GAB} . RH}{(1 - K_{GAB} . RH) . (1 - K_{GAB} . RH + C_{GAB} . K_{GAB} . RH)} \quad \text{Eq. 16}$$

where $W(RH)$ is the water content at a relative humidity, W_m is the maximum adsorbed water content, C_{GAB} is the *GAB* coefficient, and K_{GAB} is the correction factor.

	W_m	C	K
W_{ad}	0.02	7	0.86
W_{des}	0.08	200	0.68

Table 8: GAB coefficients of sorption-desorption isotherms for hemp concrete

The coefficients W_m, C_{GAB}, K_{GAB}, of a material for a reference temperature allow us to model sorption isotherms for any temperature (Staudt et al. [63]) (Eq. 16 and Eq. 17).

$$W_{ad,prim40\%}(RH) = W_{des}(40\%) + (W_{ad}(RH) - W_{ad}(40\%)) \frac{W_f - W_{des}(40\%)}{W_f - W_{ad}(40\%)} \quad \text{Eq. 17}$$

W_f: is the water content at 100% RH.

From these formulas, we deduce the real adsorption and desorption equations for the hemp concrete wall. These two equations have been implemented MATLAB to show the evolution of the water content. The numerical adsorption and desorption curves are presented in Figure **17**. This figure shows the evolution of the water content in the wall, obtained by integration of the sorption isotherm according to the GAB numerical model. In addition, the variation of the water content in hemp concrete has a strong influence on the hygrothermal properties such as thermal conductivity [64]. The characteristics of hemp concrete used in this study, based on the hygrothermal properties proposed by [62], are presented in Table **9**.

$\rho(kg.m^3)$	$\lambda(W.m^3K^{-1})$	C_p $(J.kg^{-1}K^{-1})$	K_m $(kg.m^{-1}.s^{-1}Pa^{-1})$	$C_m\,(kg.kg^{-1}Pa^{-1})$
454	0.0818+0.000276.T(°C) +0.24.W	1070	$3.71.10^{-11}$	$\frac{dW}{dHR}.\frac{1}{P_{vsat}}$

Table 9: Properties of hemp concrete introduced in MATLAB.

Based on the input parameters in the numerical study of [62], the simulation is performed in MATLAB with a uniform mesh of 100 nodes and a time step of 600s [62]. The results are shown in Figures **18** and **19**, which compare the simulated and measured variations of temperature and relative humidity at 5cm, 18cm, and 29cm in the wall. The simulation is carried out by taking W_{int} = $W_{ad,prim40\%}$ (RH_{int}) as the initial water content. The influence of temperature on the isotherms is not taken into account.

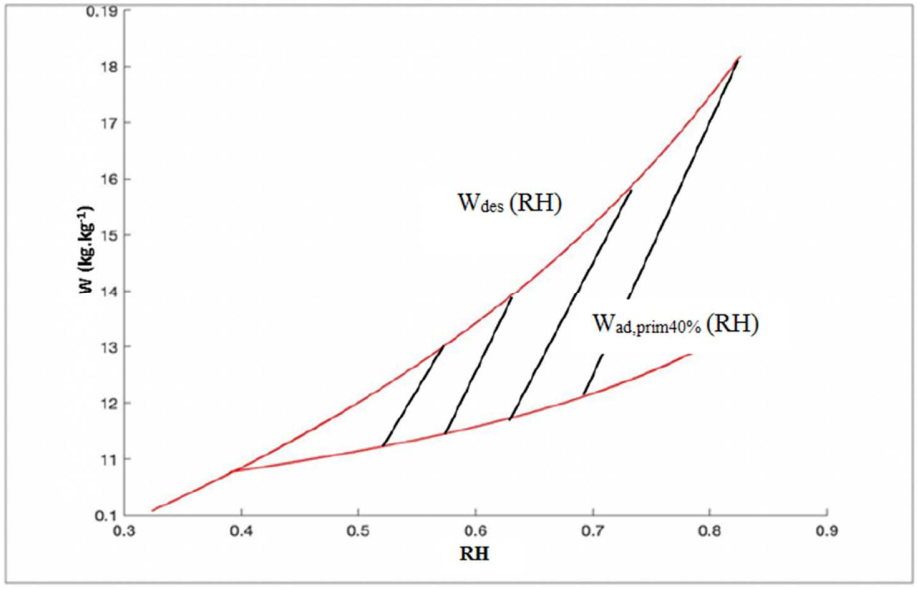

Figure 17: Sorption isotherm

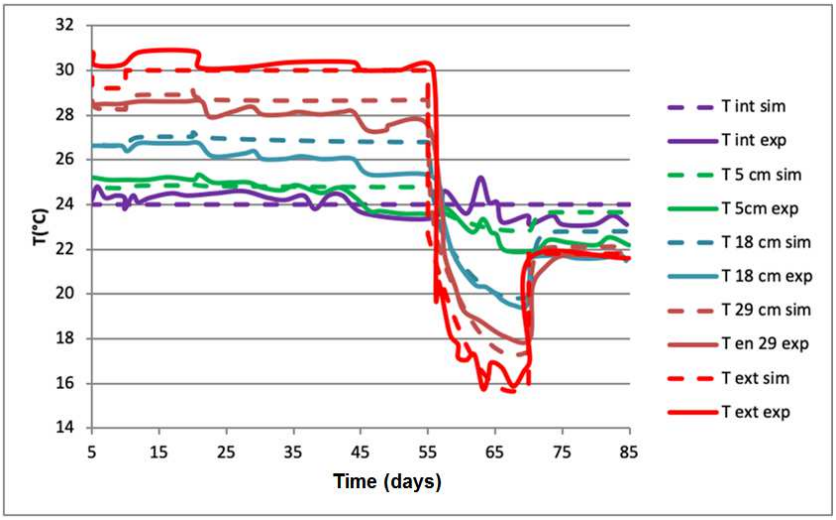

Figure 18: Simulated and measured temperature

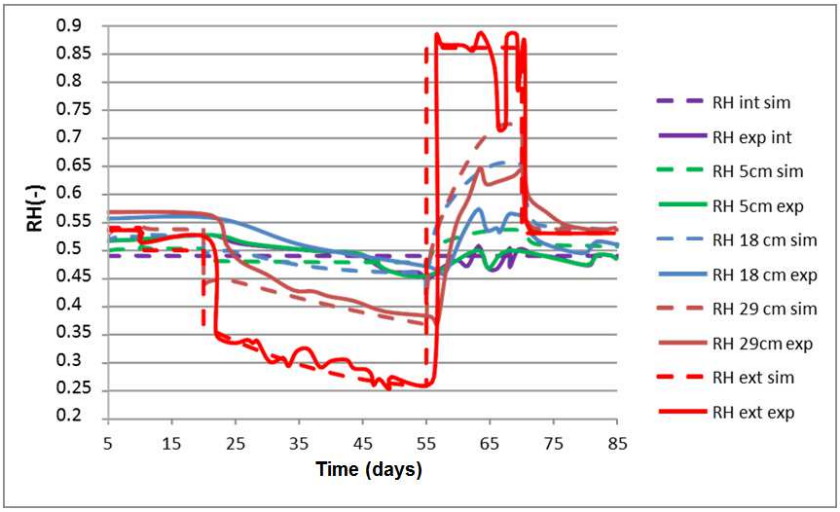

Figure 19: Simulated and measured relative humidity, taking the sorption isotherm into account.

For the second simulation in which the GAB numerical sorption model was integrated, the results showed close correspondence with the experimental results. The simulated RH profiles exhibit satisfactory agreement with the measurements. The variations of RH during the first desorption phase (between 20 and 55 days) are less significant than in the first simulation. During the second adsorption phase (between the 55th and 70th days), the simulated RH variations are greater than those measured. This is due to a sharp drop in the RH of the outside air on day 67. This drop was not taken into account in the numerical simulation. On the other hand, we observe that the thermal evolution in the wall is not impacted by taking the initial water content and variation of water content into account.

In conclusion, the sorption isotherm is an important factor in improving numerical prediction of the hygrothermal behavior of hemp concrete. In addition, our model is able to correctly predict the hygrothermal behavior of an unplastered hemp concrete wall under various climatic conditions if we estimate the correct value of the initial water content.

6. Comparison with cellular concrete

In order to test the validity of the reduced model on different building materials, a numerical study using the reduced model is carried out on cellular concrete: a conventional building material. This will extend the validity, which initially applies only to hygroscopic hemp concrete. The validation is based on the experimental work of [61], with the same configuration of hemp concrete as presented in section 4.1. **Figure 6** shows the climatic stresses of T and RH imposed by Samri. The characteristics of a 30cm-thick cellular concrete wall used in the dry state are shown in Table **10**. The simulation is performed with a 50-node mesh and a time step size of 600s.

Table 10: Properties of cellular concrete input into MATLAB [61]

ρ $(kg.m^3)$	λ $(W.m^3K^{-1})$	C_p $(J.kg^{-1}K^{-1})$	K_m $(kg.m^{-1}.s^{-1}Pa^{-1})$	$C_m\,(kg.kg^{-1}Pa^{-1})$
429.5	0.118	915.3	$2.4.10^{-11}$	$5.07.10^{-4}$

We compare the numerical and experimental results on the hygrothermal behavior of cellular concrete. The profiles of T and RH at point C (middle of the wall) are shown in **Figures 20** and **21**. It is also interesting to compare the behavior of the cellular concrete wall to the results found with hemp concrete, presented in section 4.1 (**Figures 7** and **8**), as well as the hygrothermal properties to show the superiority of hemp concrete over conventional concrete.

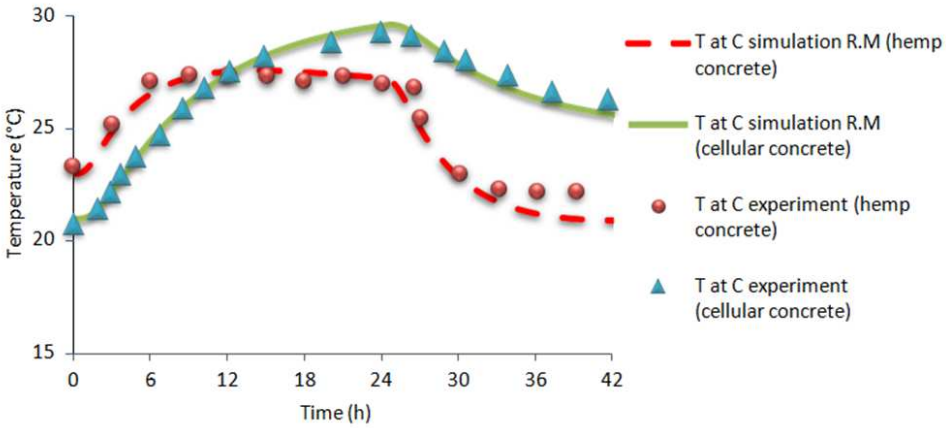

Figure 20: Comparison between experimental and numerical findings of temperature evolution at point C for hemp concrete and cellular concrete.

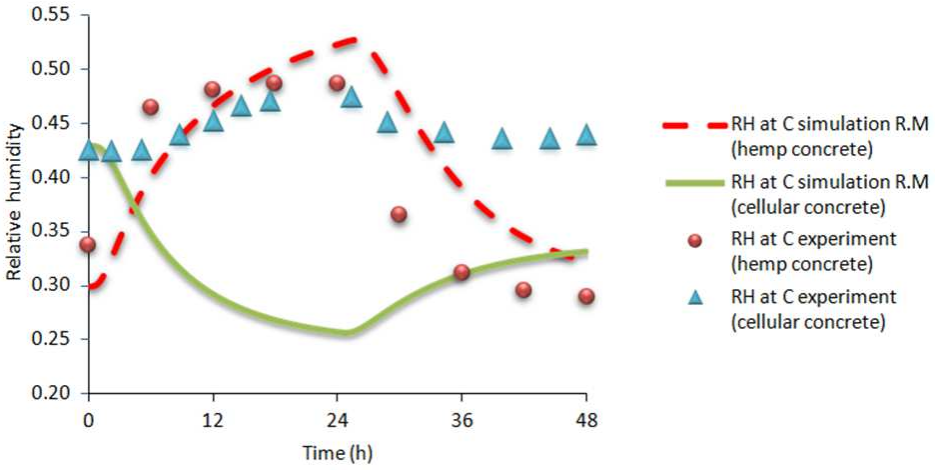

Figure 21: Comparison between the experimental and numerical findings of the evolution of relative humidity at point C for hemp concrete and cellular concrete.

The comparison between the numerical and experimental results of the temperature profile of cellular concrete at point C shows a good consistency (**Figure 20**). On the other hand, the reduced model does not correctly predict the evolution of the local relative humidity in a cellular concrete wall. There is a major deviation between the simulated and measured results, with the simulated values being much lower than those measured (**Figure 21**). This may be due to the absence of some parameters that were eliminated from the reduced model, such as the coefficient of advective heat transfer due to the vapor pressure gradient α.

In addition, the response of the cellular concrete wall is radically different from that of the hemp concrete wall. From a thermal viewpoint, the hemp concrete delays and attenuates the perception of heat inside the building. During the first six hours, the temperature of the hemp concrete rises to 27°C and remains constant for the rest of the sequence, whereas the temperature of cellular concrete continues to rise until it reaches the outdoor temperature of 30°C. Thus, during this first stage, characterized by the increasing in outdoor temperature to 30°C, an increase of vapor pressure was observed within the hemp concrete wall, resulting in evaporation. This was accompanied by heat absorption, which attenuates the temperature variations within the wall. These phenomena remain very limited in cellular concrete and therefore do not significantly influence heat transfer. This confirms that hemp concrete is a better insulator than cellular concrete, and is likely to create a greater thermal phase shift due to phase change.

From a hydric viewpoint, hemp concrete allows better circulation of relative humidity. The hemp concrete absorbs the variations in relative humidity imposed on both sides of the wall due to its

moisture absorption capacity. Hemp concrete's capacity of water regulation is greater than that of cellular concrete.

7. Numerical study of the hygrothermal behavior of a hemp concrete wall subjected to real sequences of T and RH

After validating our reduced model's overall performance on a hemp concrete wall, we analyzed the hygrothermal response of hemp concrete wall under real atmospheric conditions generally encountered in construction (summer, winter, and daily stresses). For this analysis, we used the same configuration of [62] as in section 4.2 and the same interior and initial conditions, but on the exterior side, we imposed different gradient configurations to represent summer and winter conditions. Also, we look at the evolution of T and RH over the course of a day to predict the heat and humidity flows with the day/night cycles. The simulation configuration is based on the NORDTEST experimental protocol [65].

7.1. Summer sequence study

The 36cm-thick hemp concrete wall is subjected to a numerical sequence reflecting the atmosphere generally encountered in summer, for 12 days, consisting of four stages of 72 hours each. The values taken for T and RH at each stage are shown in Table 11. The purpose of these different configurations is to highlight other drivers of water transfer that may come into play besides the vapor pressure, and evaluate its ability to redistribute the RH in the wall.

Table 11: Variations of outdoor T° and RH input into MATLAB

	Phase 1	Phase 2	Phase 3	Phase 4
Time	1<t<3d	3<t<6d	6<t<9d	T>9d
T (°C)	30	19	30	20
RH (-)	0.85	0.40	0.45	0.70
Gradient configurations	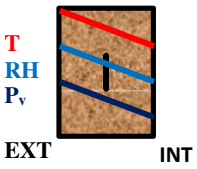	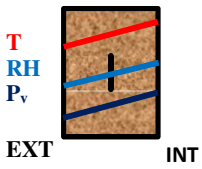	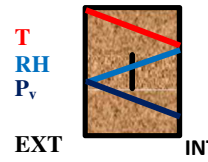	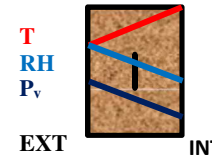

Based on the same numerical protocol (mesh and time step) used previously (section 4.2), the numerical responses of temperature and relative humidity in the three positions in the wall (5cm,18cm, and 29cm) are presented in Figures 22 and 23. These results compare the reduced model's performance with and without taking the sorption isotherm into account; the influence of the temperature on the sorption isotherm is not considered.

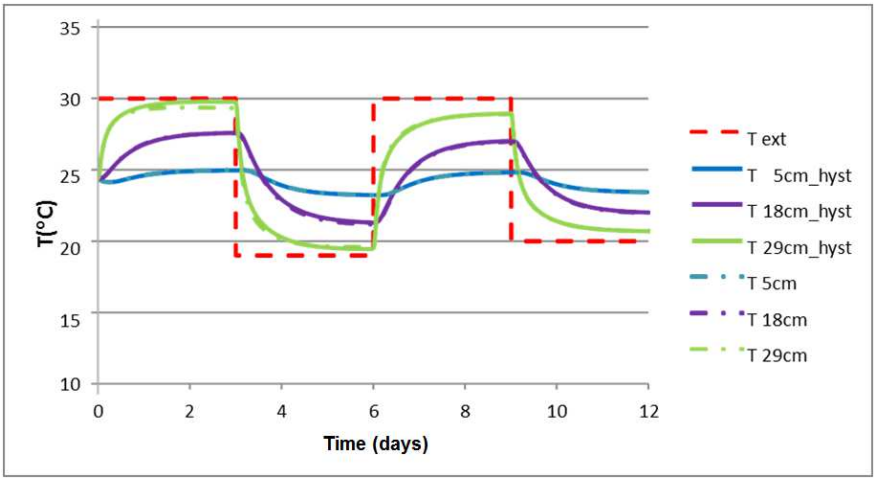

Figure 22: Comparison of simulated temperature (with and without hysteresis).

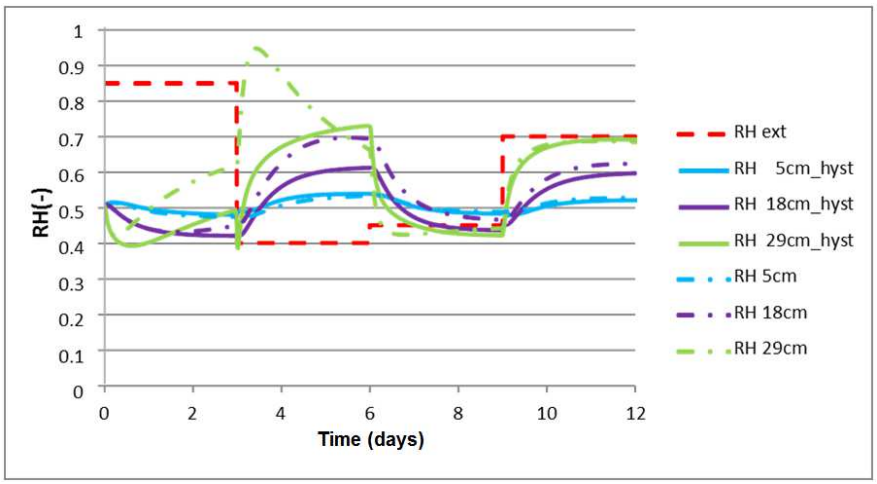

Figure 23: Comparison of simulated relative humidity (with and without hysteresis).

The temperature results showed that the temperature evolution is not affected by the sorption isotherm or the variation of the water vapor distribution in the wall. The hemp concrete is found to reduce the temperature to the greatest extent possible. Therefore, at 5cm from the internal side, the temperature oscillates between 23 and 25°.

Concerning the distributions of RH, we observe that the first two phases are strongly impacted by the numerical modeling of the water content in predicting the material's hygrothermal behavior. The first phase of adsorption is accompanied by a release of energy, generating a temperature increase at the external surface of the wall. This decreases the amount of water on the external side of the wall (at 29cm). Then, the relative humidity increases when the temperature begins to stabilize. At the end of the first phase, the RH at 29cm changes rapidly, because both the temperature and RH drop sharply. Conversely, when the evolution of the water content is not considered, we do not observe this phenomenon. This indicates an overestimation

of the storage capacity, especially in the first two phases. Therefore, it is important to take the variation of the water content into account when determining the hygrothermal properties, in order to better predict the hygrothermal behavior. In addition, the RH 5cm from the interior side is of the order of 50%, so hemp concrete is able to regulate the humidity in the building and guarantee a comfortable interior atmosphere, due to its ability to dampen external variations.

As a result, hemp concrete is able to reduce variations of humidity and temperature as far as possible, and maintain comfortable conditions in the building during summer. Moreover, the temperature governs the distribution of water content in the wall. These results highlight the importance of the dynamics of thermal transfer on water transfer.

7.2. Winter sequence study

In order to evaluate the impact of low temperature on the wall, we ran a winter sequence composed of an adsorption phase (RH=85%) and a desorption phase (RH=30%) lasting four days each, while the outside temperature is kept constant at 12°C (Table **12**). Using this stress, we can predict the influence of extreme variations of humidity on the temperature.

Table 12: Variations of external T and RH input into MATLAB.

	Phase 1	Phase 2
Time	1<t<4d	4<t<8d
T (°C)	12	12
RH (-)	0.85	0.30
Gradient configurations	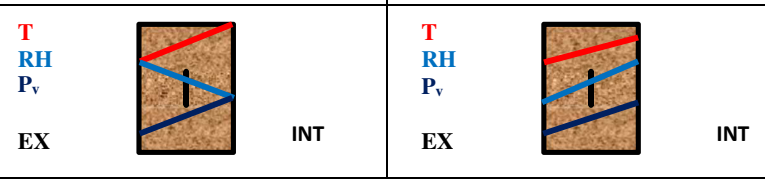	

The numerical results in terms of the hygrothermal behavior for both cases (with and without consideration of the sorption isotherm) are shown in **Figure 24** and **Figure 25**.

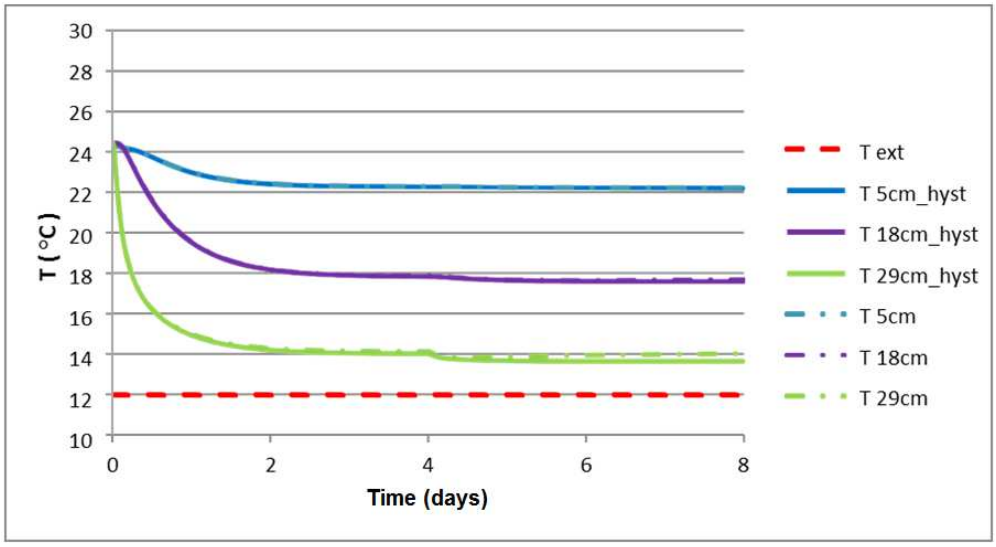

Figure 24: Comparison of simulated temperature (with and without initial water content).

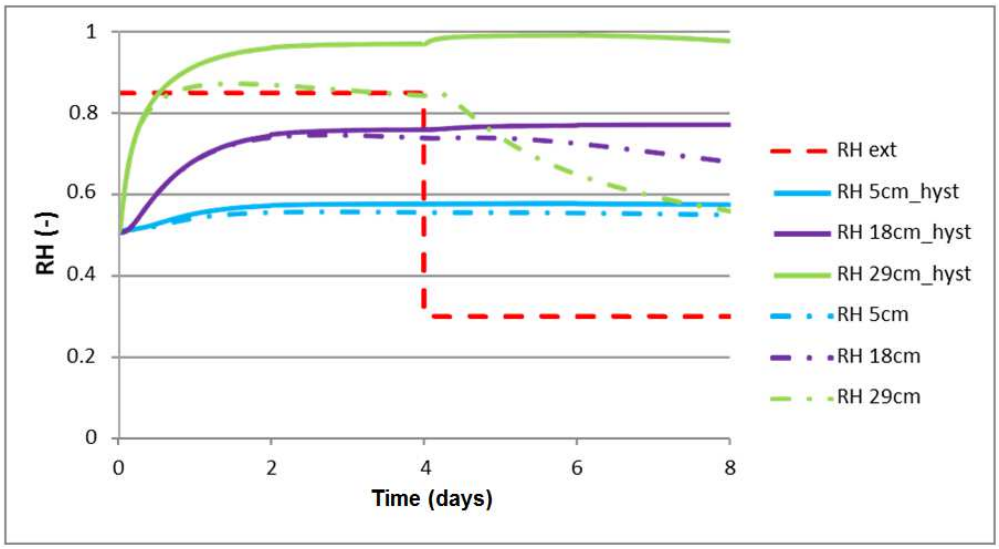

Figure 25: Comparison of simulated relative humidity (with and without initial water content).

The simulated temperatures at 18cm and 29cm reach a quasi-steady state during the cooling phase, with low values near the outer surface, whereas the temperature at the interior surface is similar to the indoor conditions. In addition, we observe that the simulated temperature is not impacted by water content, except for a slight decrease during the desorption phase at the external position. On the other hand, the evolution of relative humidity is more significant for the simulation that integrates the sorption isotherm model. The water content at 29cm increases to the point of saturation, but as we move nearer to the internal surface, it decreases progressively. Therefore, it is recommended to use a layer of plaster to avoid condensation on the external side of the wall during winter.

7.3. Daily sequence study

In accordance with the NORDTEST experimental protocol [65], the hemp concrete is subjected to 75% RH for 8 hours (night) and 33% for 16 hours (day), at a constant temperature of 23°C (**Figure 26**). This protocol is replicated on two days so as to compare and analyze the real hygrothermal behavior of hemp concrete and evaluate the influence of water content evolution on hygrothermal behavior on a daily basis. The results are shown in **Figures 27** and **28**.

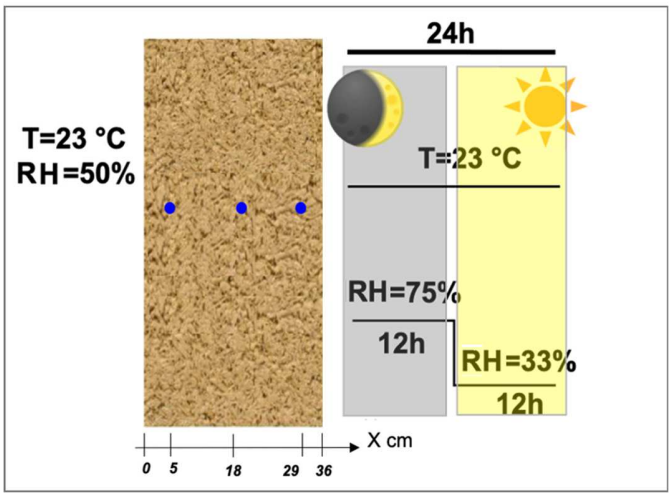

Figure 26: Configuration of wall studied for two days (24h×2).

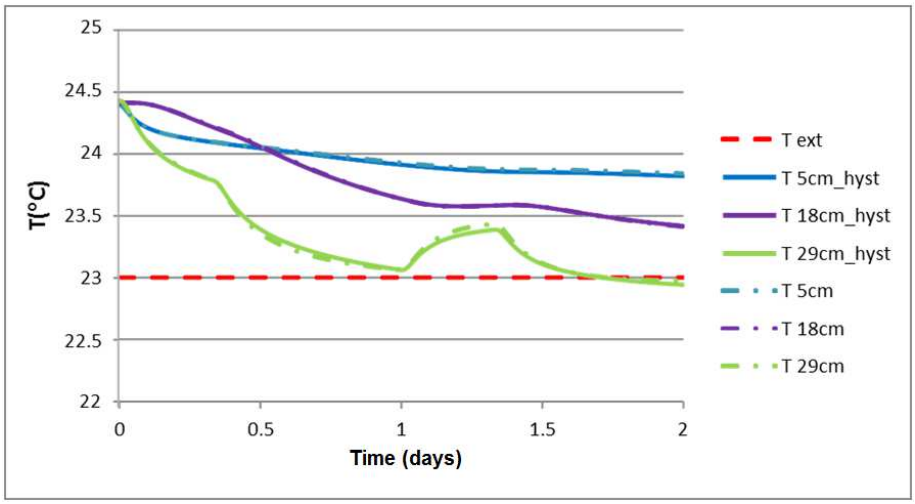

Figure 27: Comparison of simulated temperature (with and without initial water content).

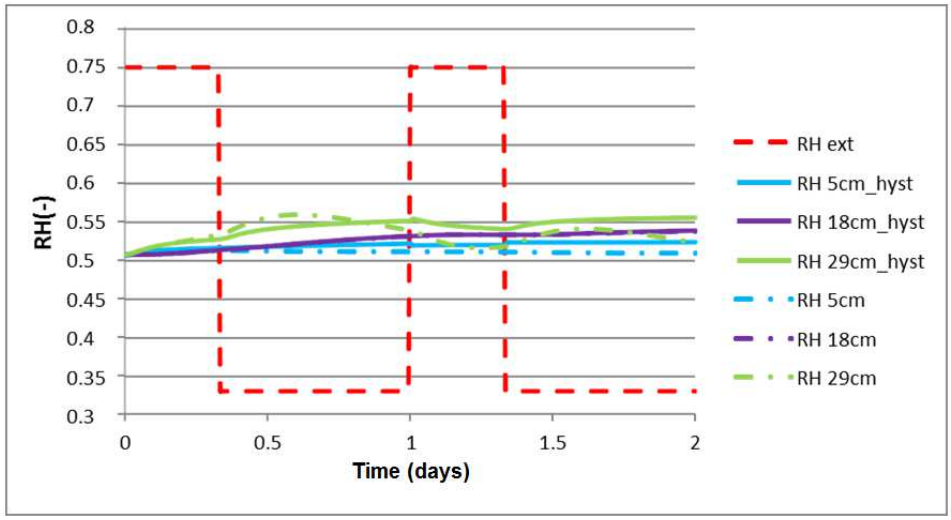

Figure 28: Comparison of simulated relative humidity (with and without initial water content).

Evidently, the temperature on the outside part of the wall is strongly influenced by variations in RH. However, such variations are greatly attenuated on the internal side, at depths of 5cm and 18cm. Moreover, temperature peaks are observed, which are due to the phase change effect. The negative peaks correspond to the desorption phase characterized by heat absorption; the positive ones represent the adsorption phase characterized by heat release.

On the other hand, for the two cases with and without integration of the numerical sorption model, the RH profile of the wall is roughly consistent in the three positions, while the outdoor relative humidity varies widely. Greater accuracy is attained when hysteresis is taken into consideration.

Therefore, hemp concrete is able to create a thermal and hydric phase shift during the day (day/night). In addition, the numerical prediction of hemp concrete's behavior requires a sound description of the hygrothermal properties as a function of the water distribution in the wall.

8. Conclusion

In this work, a sensitivity analysis was performed to study the influence of HAM model parameters on the hygrothermal transfers in a building envelope made of hemp concrete. The developed HAM model is inspired by the work of Philip and De Vries [48]. Using MATLAB, the parametric sensitivity analysis was carried out based on bounded probability density distribution according to the beta law. The analysis was based on the inflection points detected after each iteration. The correlation between parameters and driving transfer potentials (T, P_v, and P) was determined by the slope coefficient of variation of these inflection points. The results revealed the four most influential parameters on HAM transfer: thermal conductivity λ, specific heat C_p, water storage capacity C_m, and water vapor permeability K_m. Armed with this

information, we were able to develop a reduced HAM model. A dimensionless study of the reduced model was carried out. This study identified a factor which links the thermal and the hygric performances of building materials and can classify them by their behaviors. Bio-based materials are found to be ideal for optimizing building performance. In order to validate the reliability of the reduced model, the simulated results were compared to those of experiments reported in the literature. The comparison showed that the model is effective at predicting the hygrothermal behavior of a hemp concrete wall, when the evolution of water content in the wall is taken into account. On the other hand, the model failed to predict the hygric behavior of cellular concrete. In addition, this work studied the hygrothermal behaviors of a hemp concrete wall subjected to stresses generally encountered in the construction sector (winter, summer, and daily stresses). The results showed the effectiveness of hemp material in thermal insulation and moisture regulation. To ensure accurate RH predictions, the evolution of water content (hysteresis) must always be taken into account in the model.

Bibliography

[1] X. Cheng and J. Fan, "Simulation of heat and moisture transfer with phase change and mobile condensates in fibrous insulation," *International Journal of Thermal Sciences*, vol. 43, no. 7, pp. 665–676, 2004.

[2] R. Damle, O. Lehmkuhl, J. Rigola, and A. Oliva, "Combined heat and moisture transfer in buildings systems," *International High Performance Buildings Conference*, p. 72, 2012.

[3] G. H. Dos Santos and N. Mendes, "Simultaneous heat and moisture transfer in soils combined with building simulation," *Energy and Buildings*, vol. 38, no. 4, pp. 303–314, 2006.

[4] J. Eitelberger and K. Hofstetter, "A comprehensive model for transient moisture transport in wood below the fiber saturation point: Physical background, implementation and experimental validation," *International Journal of Thermal Sciences*, vol. 50, no. 10, pp. 1861–1866, 2011.

[5] S. Gasparin, J. Berger, D. Dutykh, and N. Mendes, "An adaptive simulation of nonlinear heat and moisture transfer as a boundary value problem," *International Journal of Thermal Sciences*, vol. 133, pp. 120–139, 2018.

[6] H. M. Künzel, *Simultaneous Heat and Moisture Transport in Building Components One- and two-dimensional calculation using simple parameters* . 1995.

[7] Q. Li, J. Rao, and P. Fazio, "Hygrothermal simulation of drying performance of typical north american building envelope," *In: Proceedings of the 10th conference of*

International Building Performance Simulation Association, Montreal, Canada; August 15–18., 2005.

[8] M. Louërat, M. Ayouz, and P. Perré, "Heat and moisture diffusion in spruce and wood panels computed from 3-D morphologies using the Lattice Boltzmann method," *International Journal of Thermal Sciences*, vol. 130, pp. 471–483, 2018.

[9] N. Mendes, P. C. Philippi, and R. Lamberts, "A new mathematical method to solve highly coupled equations of heat and mass transfer in porous media," *International Journal of Heat and Mass Transfer*, vol. 45, no. 3, pp. 509–518, 2002.

[10] C. R. Pedersen, "Prediction of moisture transfer in building constructions," *Building and Environment*, vol. 27, no. 3, pp. 387–397, 1992.

[11] M. Simo-Tagne, R. Rémond, Y. Rogaume, A. Zoulalian, and B. Bonoma, "Modeling of coupled heat and mass transfer during drying of tropical woods," *International Journal of Thermal Sciences*, vol. 109, pp. 299–308, 2016.

[12] G. H. dos Santos and N. Mendes, "Heat, air and moisture transfer through hollow porous blocks," *International Journal of Heat and Mass Transfer*, vol. 52, pp. 2390–2398, 2009.

[13] Q. Li, J. Rao, and P. Fazio, "Development of HAM tool for building envelope analysis," *Building and Environment*, vol. 44, pp. 1065–1073, 2009.

[14] L. Ayres de Mello, L. M. Moura, and N. Mendes, "A model for predicting heat, air and moisture transfer through fibrous materials," *International Journal of Thermal Sciences*, vol. 145, p. 106036, 2019.

[15] L. Ayres De Mello, L. M. Moura, and N. Mendes, "A model for assessment of heat and moisture transfer through hollow porous buildings elements," *Case Studies in Thermal Engineering*, vol. 14, p. 100446, 2019.

[16] C. Belleudy, M. Woloszyn, M. Chhay, and M. Cosnier, "A 2D model for coupled heat, air, and moisture transfer through porous media in contact with air channels," *International Journal of Heat and Mass Transfer*, vol. 95, pp. 453–465, 2016.

[17] R. Liu and Y. Huang, "Heat and moisture transfer characteristics of multilayer walls," *Energy Procedia*, vol. 152, pp. 324–329, 2018.

[18] B. Remki, K. Abahri, M. Tahlaiti, and R. Belarbi, "Hygrothermal transfer in wood drying under the atmospheric pressure gradient," *International Journal of Thermal Sciences*, vol. 57, pp. 135–141, 2012.

[19] J. Berger, D. Dutykh, N. Mendes, and B. Rysbaiuly, “A new model for simulating heat, air and moisture transport in porous building materials,” *Engineering Reports. 2020; e12099.*.

[20] F. Mnasri, K. Abahri, M. El Ganaoui, R. Bennacer, and S. Gabsi, “Numerical analysis of heat, air, and moisture transfers in a wooden building material,” *Thermal Science*, vol. 21, no. 2, pp. 785–795, 2017.

[21] T. Z. Desta, J. Langmans, and S. Roels, “Experimental data set for validation of heat, air and moisture transport models of building envelopes,” *Building and Environment*, vol. 46, no. 5, pp. 1038–1046, 2011.

[22] J. Langmans, A. Nicolai, R. Klein, and S. Roels, “A quasi-steady state implementation of air convection in a transient heat and moisture building component model,” *Building and Environment*, vol. 58, pp. 208–218, 2012.

[23] L. Škerget, A. Tadeu, and J. Ravnik, “BEM numerical simulation of coupled heat, air and moisture flow through a multilayered porous solid,” *Engineering Analysis with Boundary Elements*, vol. 74, pp. 24–33, 2017.

[24] F. Tariku, K. Kumaran, and P. Fazio, “Integrated analysis of whole building heat, air and moisture transfer,” *International Journal of Heat and Mass Transfer*, vol. 53, pp. 3111–3120, 2010.

[25] S. J. Chang and S. Kim, “Hygrothermal performance of exterior wall structures using a heat, air and moisture modeling,” *Energy Procedia*, vol. 78, pp. 3434–3439, 2015.

[26] N. Mendes, F. C. Winkelmann, R. Lamberts, and P. C. Philippi, “Moisture effects on conduction loads,” *Energy and Buildings*, vol. 35, pp. 631–644, 2003.

[27] M. Bart, S. Moissette, Y. A. Oumeziane, and C. Lanos, “Transient hygrothermal modelling of coated hemp-concrete walls,” *European Journal of Environmental and Civil Engineering*, vol. 18, no. 8, pp. 927–944, 2014, doi: 10.1080/19648189.2014.911122.

[28] S. O. Olutimayin and C. J. Simonson, “Measuring and modeling vapor boundary layer growth during transient diffusion heat and moisture transfer in cellulose insulation,” *International Journal of Heat and Mass Transfer*, vol. 48, pp. 3319–3330, 2005.

[29] M. Van Belleghem, H. J. Steeman, M. Steeman, A. Janssens, and M. De Paepe, “Sensitivity analysis of CFD coupled non-isothermal heat and moisture modelling,” *Building and Environment*, vol. 45, pp. 2485–2496, 2010.

[30] Y. Aït Oumeziane, S. Moissette, M. Bart, F. Collet, S. Pretot, and C. Lanos, "Influence of hysteresis on the transient hygrothermal response of a hemp concrete wall," *Journal of Building Performance Simulation*, vol. 10, pp. 256–271, 2017.

[31] I. Othmen, P. Poullain, and N. Leklou, "Sensitivity analysis of the transient heat and moisture transfer in a single layer wall," *European Journal of Environmental and Civil Engineering*, vol. 24, pp. 2211–2229, 2018.

[32] T. Defraeye, B. Blocken, and J. Carmeliet, "Influence of uncertainty in heat-moisture transport properties on convective drying of porous materials by numerical modelling," *Chemical Engineering Research and Design*, vol. 91, no. 1, pp. 36–42, 2013.

[33] M. Steeman, M. Van Belleghem, M. De Paepe, and A. Janssens, "Experimental validation and sensitivity analysis of a coupled BES-HAM model," *Building and Environment*, vol. 45, pp. 2202–2217, 2010.

[34] A. Andrianandraina, P. Poullain, B. Cazacliu, and A. Ventura, "SENSITIVITY ANALYSIS OF PARAMETERS INFLUENCING BUILDING HEATING ENERGY CONSUMPTION USING HEMP-LIME MATERIAL," *Academic Journal of Civil Engineering*, vol. 33, no. 2, pp. 687–694, 2015.

[35] D. Garcia Sanchez, B. Lacarrière, M. Musy, and B. Bourges, "Application of sensitivity analysis in building energy simulations: Combining first- and second-order elementary effects methods," *Energy and Buildings*, vol. 68, pp. 741–750, 2014.

[36] J. Goffart, M. Rabouille, and N. Mendes, "Uncertainty and sensitivity analysis applied to hygrothermal simulation of a brick building in a hot and humid climate," *Journal of Building Performance Simulation*, vol. 10, pp. 37–57, 2015.

[37] E. Stéphan, R. Cantin, A. Caucheteux, S. Tasca-Guernouti, and P. Michel, "Experimental assessment of thermal inertia in insulated and non-insulated old limestone buildings," *Building and Environment*, vol. 80, pp. 241–248, 2014.

[38] T. Alioua, B. Agoudjil, A. Boudenne, and K. Benzarti, "Sensitivity analysis of transient heat and moisture transfer in a bio-based date palm concrete wall," *Building and Environment*, vol. 202, p. 108019, 2021.

[39] A. D. Tran Le, C. Maalouf, T. H. Mai, E. Wurtz, and F. Collet, "Transient hygrothermal behaviour of a hemp concrete building envelope," *Energy and Buildings*, vol. 42, pp. 1797–1806, 2010.

[40] J. Kwiatkowski, M. Woloszyn, and J. J. Roux, "Modelling of hysteresis influence on mass transfer in building materials," *Building and Environment*, vol. 44, pp. 633–642, 2009.

[41] S. Pinich, M. Taheri, U. Kingdom, and A. Mahdavi, "Sensitivity analysis of the hygro-thermal simulation model of a historical building's facade in a hot-humid climate," *Conference: BauSIM2018 - 7th IBPSA Germany/AustriaAt: Karlsruhe, Germany*, 2018.

[42] A. H. Holm, H. M. Kuenzel, and J. Radon, "Uncertainty approaches for hygrothermal building simulations—drying of AAC in hot and humid climates," *Thermal Performance of the Exterior Envelopes of Whole Buildings*, pp. 1–6, 2001.

[43] G. Xing-Guo, L. Hongtao, Z. Jingxin, L. Xiang-Wei, and C. Guo-Jie, "Sensitivity Analysis applied to Hygrothermal Simulation of a Brick Building in Hot and Humid Climate," *Procedia Engineering*, vol. 205, pp. 665–671, 2017.

[44] B. Seng, S. Lorente, and C. Magniont, "Scale analysis of heat and moisture transfer through bio-based materials — Application to hemp concrete," *Energy and Buildings*, vol. 155, pp. 546–558, Nov. 2017, doi: 10.1016/j.enbuild.2017.09.026.

[45] B. Seng, C. Magniont, S. Gallego, and S. Lorente, "Behavior of a hemp-based concrete wall under dynamic thermal and hygric solicitations," *Energy and Buildings*, vol. 232, Feb. 2021, doi: 10.1016/j.enbuild.2020.110669.

[46] A. v Luikov, "System of differential equation of heat and mass transfer in capillary porous bodies."

[47] S. Whitaker, "Simultaneous Heat, Mass, and Momentum Transfer in Porous Media: A Theory of Drying," *Advances in Heat Transfer*, vol. 13, no. C, pp. 119–203, Jan. 1977, doi: 10.1016/S0065-2717(08)70223-5.

[48] J. R. Philip and D.A. De Vries, "Moisture Movement in Porous Materials under Temperature Gradients," *Transactions, American Geophysical Union*, vol. Vol. 38, N. 2, 1957.

[49] H. M. Künzel, *Simultaneous heat and moisture transport in building components : one- and two-dimensional calculation using simple parameters*. IRB Verlag, 1995.

[50] H. Janssen, B. Blocken, and J. Carmeliet, "Conservative modelling of the moisture and heat transfer in building components under atmospheric excitation," *International Journal of Heat and Mass Transfer*, vol. 50, no. 5–6, pp. 1128–1140, Mar. 2007, doi: 10.1016/j.ijheatmasstransfer.2006.06.048.

[51] Hagentoft C.E., “Hamstad WP2 benchmark package, Final report : methodology of HAM modeling.” Chalmers University of Technology, Suède., 2002.

[52] Y. A. Oumeziane, “Evaluation des performances hygrothermiques d’une paroi par simulation numérique: application aux parois en béton de chanvre,” *Thèse, Génie civil. INSA de Rennes*, 2013.

[53] K. Abahri, R. Bennacer, and R. Belarbi, “Sensitivity analyses of convective and diffusive driving potentials on combined heat air and mass transfer in hygroscopic materials,” *Numerical Heat Transfer; Part A: Applications*, vol. 69, pp. 1079–1091, 2016.

[54] M. Qin, R. Belarbi, A. Ait-Mokhtar, and L. O. Nilsson, “Nonisothermal moisture transport in hygroscopic building materials: Modeling for the determination of moisture transport coefficients,” *Transport in Porous Media*, vol. 72, pp. 255–271, 2008.

[55] J. Zueco and L. M. López-Ochoa, “Network numerical simulation of coupled heat and moisture transfer in capillary porous media,” *International Communications in Heat and Mass Transfer*, vol. 44, pp. 1–6, 2013.

[56] R. Younsi, D. Kocaefe, and Y. Kocaefe, “Three-dimensional simulation of heat and moisture transfer in wood,” *Applied Thermal Engineering*, vol. 26, pp. 1274–1285, 2006.

[57] L. B. Dantas, H. R. B. Orlande, and R. M. Cotta, “Estimation of dimensionless parameters of Luikov’s system for heat and mass transfer in capillary porous media,” *International Journal of Thermal Sciences*, vol. 41, pp. 217–227, 2002.

[58] J. Berger, C. Legros, and M. Abdykarim, “Dimensionless formulation and similarity to assess the main phenomena of heat and mass transfer in building porous material,” *Journal of Building Engineering*, vol. 35, p. 101849, 2020.

[59] L. B. Dantas, H. R. B. Orlande, and R. M. Cotta, “Improved lumped-differential formulations and hybrid solution methods for drying in porous media,” *International Journal of Thermal Sciences*, vol. 46, pp. 878–889, 2007.

[60] A. Trabelsi, Z. Slimani, and J. Virgone, “Response surface analysis of the dimensionless heat and mass transfer parameters of Medium Density Fiberboard,” *International Journal of Heat and Mass Transfer*, vol. 127, pp. 623–630, 2018.

[61] D. Samri, “Analyse physique et caractérisation hygrothermique des matériaux de construction : approche expérimentale et modélisation numérique - Thèse de doctorat, Ecole Nationale des Travaux Publics de l’Etat (ENTPE),” 2008.

[62] D. Lelièvre, “Simulation numérique des transferts de chaleur et d ’ humidité dans une paroi multicouche de bâtiment en matériaux biosourcés,” 2015.

[63] P. B. Staudt, I. C. Tessaro, L. D. F. Marczak, R. D. P. Soares, and N. S. M. Cardozo, “A new method for predicting sorption isotherms at different temperatures : Extension to the GAB model,” *Journal of Food Engineering*, vol. 118, no. 3, pp. 247–255, 2013.

[64] F. Collet, “Caractérisation hydrique et thermique de matériaux du génie civil à faibles impacts environnementaux. Thèse de doctorat génie civil. INSA de Rennes,” 2004.

[65] C. Rode *et al.*, “NORDTEST Project on Moisture Buffer Value of Materials,” *In AIVC 26th conference: Ventilation in relation to the energy performance of buildings. Air Infiltration and Ventilation*, pp. 47–52, 2005.